ELSEVIER

Physica D 73 (1994) 318–334

PHYSICA D

Synchronized disorder in a 2D complex Ginzburg–Landau equation

M. Bazhenov, M. Rabinovich

Institute of Applied Physics, Russian Academy of Science, 46 Uljanov Str., 603600 Nizhny Novgorod, Russian Federation

Received 29 November 1993; accepted 13 December 1993; communicated by B.V. Chirikov

Abstract

The phenomenon of spiral pair synchronization by oscillating strips (Nozaki–Bekki solution) in a 2D CGLE is investigated analytically. The equations describing the interaction of the strips with one another and with spirals are derived. Analysis of the equations shows that under certain conditions the strips lead to frequency and phase locking of the spirals. In this case the spiral pair (dipole) is aligned parallel to the strips, with the position along the strips being arbitrary. Thus, the interaction with strips may transform the spatio-temporal chaos of spirals to the regime of periodically oscillating spatial disorder. The dynamics of circular strips is investigated and their lifetime is estimated. The behavior of the spirals bounded by circular stript is analysed.

1. Introduction

A broad variety of regimes existing in a CGLE is sometimes puzzling. By now thorough investigations have been performed on cylindrical and plane waves [4,5], hole solutions [2,3,6–10], various spirals [11–23], vortex lines [24], phase and amplitude turbulence [25–30], defect mediated turbulence [31–33], spatial disorder periodically varying in time [34–35], and many others (we can also refer the reader to [36–44]). What is this remarkable richness of behaviour accounted for? We believe that physically it is explained by exceptional diversity of synchronization phenomena and of the ways they manifest themselves. Indeed, bearing in mind that a two-dimensional nonequilibrium medium described by a CGLE can be considered as an ensemble of coupled generators whose frequency depends on the amplitude of oscillations, we can interpret many regimes as simple or complex dynamics of the frequency or phase locking fronts of coupled elements of the medium. This language may also be used to explain an extraordinary stability of single spirals, as well as the existence of localized turbulent spots [1]. Here we will investigate the phenomenon of locking at interaction of the structures having different topologies within a two-dimensional CGLE. Namely, we will analyse the interaction of extended holes with spiral pairs, or dipoles which can be considered as elementary objects among a broad variety of solutions to a two-dimensional CGLE.

0167-2789/94/$07.00
SSDI 0167-2789(93)E0340-H

A new class of regimes was revealed in the frames of a two-dimensionl CGLE analytically and by means of computer experiment. It is time-synchronized spatial disorder of dipoles.

Let us write the Ginzburg–Landau equation in the form

$$\partial_t a = a + (1 + \mathrm{i}\alpha)\nabla^2 a - (1 + \mathrm{i}\beta)|a|^2 a. \tag{1}$$

The solution in the form of a single spiral can be written as

$$a_0 = F(r)\exp[-\mathrm{i}\omega t + im\varphi + \mathrm{i}\theta(r)], \tag{2}$$

where (r, φ) are the polar coordinates, m is the topological charge, and $\omega = (\alpha - \beta)Q^2 + \beta$. The constant Q is an asymptotic wavenumber of spiral-radiated waves that is determined by the parameters α and β [45]. Eq. (2) describes an m-armed spiral but only solutions with $m = \pm 1$ are stable [45]. The asymptotic expressions

$$F(r) = (1 - Q^2)^{1/2} - \frac{(1 + \alpha^2)Q}{2(1 - Q^2)^{1/2}(\alpha - \beta)} r^{-1} + \mathcal{O}(r^{-2}) \tag{3}$$

and

$$\theta(r) = Qr + \frac{1 + \alpha\beta}{2(\alpha - \beta)} \ln(r) + \mathcal{O}(r^{-1}) \tag{4}$$

are valid for the functions $F(r)$ and $\theta(r)$ at $r \gg 1$.

Another important solution to the 2D CGLE is a one-dimensional strip that has an uniform structure along one spatial coordinate and a hole structure along the other:

$$a_1 = A(x)\exp[-\mathrm{i}\omega t + \mathrm{i}\theta(x)]. \tag{5}$$

The amplitude $A(x)$ and phase $\theta(x)$ satisfy the equations

$$A(x) = \sqrt{1 - Q^2}\tanh(kx), \tag{6}$$

$$\frac{\mathrm{d}\theta}{\mathrm{d}x} = -Q\tanh(kx), \tag{7}$$

where Q is an asymptotic wavenumber that is related to frequency as $\omega = (\alpha - \beta)Q^2 + \beta$ and depends on the parameters α and β: $Q = (2k^2 - 1)/3k\alpha$. The quantity $1/k$ describes the width of the strip and k meets the equation:

$$[4(\beta - \alpha) + 18\alpha(1 + \alpha^2)]k^4 - [4(\beta - \alpha) + 9\alpha(1 + \alpha\beta)]k^2 + (\beta - \alpha) = 0.$$

The solution (5)–(7) is a trivial extension to a two-dimensional case of the hole solution that was first obtained by Nozaki and Bekki for a one-dimensional CGLE [2,3]. Stability of the solution (5) in a definite region of the parameters of relatively small and finite perturbations of a two-dimensional medium with boundary conditions periodic with respect to y was demonstrated numerically and analytically in [1].

The interaction of spiral structures – the solutions (2) to the CGLE in a two-dimensional medium – was investigated in detail in [13,17,20,21]. In this paper we will consider the effects of interactions of one-dimensional strips (5) with one another and with spirals and will attempt to explain the phenomenon of spiral synchronization by the strip field observed in numerical experiment [1]. We will also show that, besides the structures of the form (5), quasi-one-dimensional cylindrical strips (that are uniform along the angular coordinate and have a hole structure over radius) may exist for rather a long time in a two-dimensional medium. The lifetime of such strips will be estimated.

The architecture of the paper is as follows. In Section 2 spirals and strips are described in terms of a linearized phase equation and the interaction of strips with one another is considered. The collective dynamics of spirals and strips is investigated in Section 3. It is shown that in the presence of strips the spirals are phase and frequency locked and are ordered in space relative to the strips. Results of numerical investigation of the dynamics of a large ensemble of spirals and strips in a square region and in a long band are discussed in Section 4. Finally, Section 5 is concerned with analysis of the behavior of circular strips.

2. The problem of localization of solutions

Consider Eq. (1) in the region $\Omega_\infty = \{-\infty < x < \infty, -\infty < y < \infty\}$ that is unbounded along both coordinates. The asymptotic form of the solutions (2) and (5) in Ω_∞ can readily be found for two limiting cases. As $r \to \infty$, the solution (2) (or (5)) tends asymptotically to the solution in the form of a spiral (plane) wave with wavenumber Q and amplitude $\sqrt{1-Q^2}$. On the other hand, when $r \to 0$, we have $F(r) \sim r$, $\theta(r) \sim r$ ($A(x) \sim x$, $\theta(x) \sim x$). The solution (2) ((5)) has a singularity at the point $r = 0$ (on the $x = 0$ curve): the field amplitude vanishes to zero and the phase is not defined. Thus, the amplitude of the solution (2) ((5)) changes significantly only in the core region and tends to a constant value as $r \to \infty$ ($x \to \infty$). Alternatively, the variations of phase ($\nabla \arg(a)$) for the solutions (2) and (5) are not localized in space and are present arbitrarily far from the core region. Mathematically, this is manifested in that the solutions (2), (5) are unbounded in the sense of the integral norm $\| a \|_\infty^2 = \int_{\Omega_\infty} |a|^2 \, d^2 r$. This situation creates certain difficulties for analysis of the interaction of structures because the superposition principle does not hold when the structures are spaced arbitrarily far from one another.

In order to overcome this difficulty we will employ the following procedure [13]. We will set in (1) $a = Ae^{i\psi - i\omega t}$, where ω is a parameter, and assume that the amplitude A changes slowly in space and time. Under these suppositions we find [46,47]

$$A^2 = 1 - (\nabla\psi)^2 - \alpha\nabla^2\psi \tag{8}$$

$$\partial_t\psi = \omega - \beta + (1 + \alpha\beta)\nabla^2\psi + (\beta - \alpha)(\nabla\psi)^2 \tag{9}$$

Eqs. (8), (9) give a correct description of the structure of the solutions (2), (5) throughout the space except the core region. Consider Eq. (9). By employing the Hopf–Cole transformation

$$\psi = -\ln(w)/c, \quad c = \frac{\alpha - \beta}{1 + \alpha\beta}, \tag{10}$$

we obtain the linear equation

$$\partial_t w = (1 + \alpha\beta)[\nabla^2 w - B^2 w], \tag{11}$$

where $B^2 = (\alpha - \beta)(\omega - \beta)/(1 + \alpha\beta)^2$. Choosing $\omega = (\alpha - \beta)Q^2 + \beta$ we have $B = |cQ|$. Eq. (11) may be written in a gradient form

$$\partial_t w = -\frac{\delta V}{\delta w} \tag{12}$$

$$V = \frac{1+\alpha\beta}{2} \int_{\Omega_\infty} [(\nabla w)^2 + B^2 w^2]\, \mathrm{d}^2 \boldsymbol{r}, \tag{13}$$

where the functional V decreases along the trajectory of the system ($dV/dt = -\int_{\Omega_\infty} |\partial_t w|^2 \,\mathrm{d}^2\boldsymbol{r} < 0$).

Now consider the spiral solution (2) and the strip solution (5) to Eq. (1) in the new variables. For a single spiral (2) with a topological charge m we have

$$w_0 = e^{-cm\varphi} \overline{w}_0(r) \tag{14}$$

By using (4) we can readily obtain an asymptotic expression for the function $\overline{w}_0(r)$:

$$\overline{w}_0(r) = e^{-Br} \frac{1}{\sqrt{Br}} [1 + \mathcal{O}(1/Br)] \tag{15}$$

Apparently, the solution (14), (15) to (11) is localized in space and $\| w_0 \|_\infty < \infty$. The expression for the strip solution (5) upon transformation will take on the form

$$w_1 = \overline{w}_1(x), \quad \overline{w}_1(x) = [ch(kx)]^{-B/k} \tag{16}$$

The solution (16) has a uniform structure along the y-coordinate and remains nonlocalized in Ω_∞ because $\| w_1 \|_\infty = \infty$. However, the solution (16) decays exponentially along the x-coordinate and, consequently, the superposition principle is valid for analysis of the spiral–strip interaction on appropriate transformation of solutions to the form (14)–(16). Besides, formal difficulties may be surmounted by considering (1) not in Ω_∞ but, instead, in the region $\Omega = \{-\infty < x < \infty,\ 0 \le y \le L_y\}$ where $1 \ll L_y < \infty$. Then, we will have $\| w_1 \|^2 = \int_\Omega |w_1|^2 \,\mathrm{d}^2\boldsymbol{r} < \infty$.

This approach that implies passing over from (1) to (11) was used in [13] in the analysis of the interaction of two isolated spirals. It was shown, in particular, that the energy of spiral interaction is an alternating function of the distance between them and may have a local minimum to which corresponds a stable state of a pair of spirals spaced R_0 = const apart. For the spirals having opposite topological charges, the center of mass of such a system moves with a constant velocity in the direction perpendicular to the line connecting their cores. The equilibrium state R_0 between the spirals depends on the parameters α and β. In what will follow we will use (11)–(13) for analysis of a new phenomenon – forced frequency and phase locking of the spirals and their arrangement in space under the action of strip field.

Prior to analysis of cooperative dynamics of spirals and strips consider the interaction of two parallel strips with one another in the region Ω. The corresponding solution may be represented as

$$w = \overline{w}_1(|x - x_1|)\, \mathrm{e}^{\psi_1} + \overline{w}_1(|x - x_2|)\, \mathrm{e}^{\psi_2}, \tag{17}$$

where x_1 and x_2 are the coordinates of the centers of the strips while ψ_1 and ψ_2 are the phase corrections. Note that the solution (17) describes correctly the shock that separates the fields of two strips (see, e.g., [6] and the cited literature). On substitution of (17) into (13) we find

$$V = \varepsilon_1 \,\mathrm{e}^{2\psi_1} + \varepsilon_1 \,\mathrm{e}^{2\psi_2} + \varepsilon_{12} \,\mathrm{e}^{\psi_1 + \psi_2} \tag{18}$$

Here ε_1 is the self-energy of the strip:

$$\varepsilon_1 = L_y \frac{1+\alpha\beta}{2} \int_{-\infty}^{+\infty} [(\partial_x \overline{w}_1)^2 + B^2 \overline{w}_1^2]\, \mathrm{d}x, \tag{19}$$

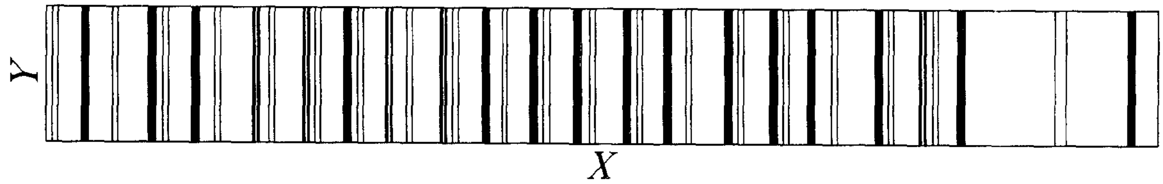

Fig. 1. Level lines of the amplitude of established field distribution for $\beta = 2$ and $\alpha = 0.2$ in the 600×80 band. A random position of the strips relative to one another that is conserved at long times indicates a very weak interaction of the strips.

with integration performed along the line $x \in (-\infty, +\infty)$, except the narrow region of width $2d_1$ in the neighborhood of the core of the strip where Eqs. (8), (9) are no longer valid. Let us find an expression for the energy of interaction ε_{12}. We will suppose that the strips are spaced rather far apart ($B|x_1 - x_2| \gg 1$) and $x_2 > x_1$. Taking into account that the integral vanishes to zero in the region between the strips we have

$$\varepsilon_{12} \cong 2L_y B^2(1+\alpha\beta) \int_{x_2+d_1}^{+\infty} \overline{w}_1(x-x_1)\,\overline{w}_1(x-x_2)\,[\tanh(k(x-x_1))\tanh(k(x-x_2))+1]\,\mathrm{d}x$$
$$\cong 2^{2B/k+1} L_y B(1+\alpha\beta)\exp[-B(x_2-x_1)]. \tag{20}$$

One can see from (20), to an acuracy of the accepted approximations, that the interaction between parallel strips is repulsive and exponentially small. The result obtained agrees well with numerical experiments. Eq. (20) was integrated by a pseudo-spectral method [48] based on FFT with periodic boundary conditions. The integration domain was taken in the form of a 600×80 band with 2048×128 or 1024×128 FFT harmonics. Results of integration for the values of the parameters $\alpha = 0.2$ and $\beta = 2$ are presented in Fig. 1. Random relative position of the strips in the band indicates weak interaction between the strips. It follows from (20) that the energy of interaction ε_{12} grows linearly as L_y increases. Therefore it can be expected that the increase of L_y will result in the increase of the average distance between the strips in a box with periodic boundary conditions. However, we cannot verify this supposition experimentally because the interaction is exponentially weak.

3. The spiral–strip interaction

We will carry out our analysis in the frame of the linear equations (11), as before. Let us restrict the number of spirals to two and represent the solution as a superposition of the fields (14)–(16) corresponding to the interacting structures:

$$w = \overline{w}_1(|x-x_1|)\,\mathrm{e}^{\psi_1} + \overline{w}_{01}(|\boldsymbol{r}-\boldsymbol{r}_{01}|)\,\mathrm{e}^{-cm_1\varphi_{01}+\psi_{01}} + \overline{w}_{02}(|\boldsymbol{r}-\boldsymbol{r}_{02}|)\,\mathrm{e}^{-cm_2\varphi_{02}+\psi_{02}}\,. \tag{21}$$

Here φ_{0i} is the angle measured relative to the spiral core with the coordinate $\boldsymbol{r}_{0i} = (x_{0i}, y_{0i})$ and x_1 is the coordinate of the core of the strip. It should be noted that the constants B entering the expressions for $\overline{w}_1$ and $\overline{w}_{0i}$ (see (15), (16)) are different, in general, because the frequency ω and the asymptotic wavenumber Q are different for isolated strips and spirals. We will be interested in the synchronization regime when the oscillating strip "imposes" its frequency on the spiral. Numerical experiment confirms that such a regime may be stable. Partial synchronization in the form of frequency mismatch is taken into account by time-dependent phase corrections ψ_1, ψ_{01}, and ψ_{02} in (21).

Let us write the functional (13) on the solution (21), like for interacting strips, in the form

$$V = \varepsilon_1 e^{2\psi_1} + \varepsilon_0 e^{2\psi_{01}} + \varepsilon_0 e^{2\psi_{02}} + \varepsilon_{101} e^{\psi_1+\psi_{01}} + \varepsilon_{102} e^{\psi_1+\psi_{02}} + \varepsilon_{012} e^{\psi_{01}+\psi_{02}}, \tag{22}$$

where ε_0 is the self-energy of the spiral that depends neither on L_y nor on the sign of the topological charge $m_i = \pm 1$, ε_1 is the self-energy of the strip depending linearly on L_y (see (19)), ε_{10i} is the energy of interaction of the strip and the ith spiral, and ε_{012} is the energy of interaction of spirals with one another. Let us assume that the spiral and the strip are spaced rather far apart and replace the integral over the entire domain by the integral over some neighborhoods of the spiral and strip cores. Then we will estimate the expression for ε_{10i} as

$$\varepsilon_{10i} = D\, e^{-B|x_1 - x_{0i}|}, \quad i = 1,2. \tag{23}$$

The character of the strip–spiral interaction does not depend on the topological charge $m_i = \pm 1$ and the energy of interaction tends exponentially to zero as the distance between the structures increases. The constant D, in particular, is determined by the contributions of the spiral and strip cores and cannot be found analytically in the framework of our approximation.

Assume that as a result of the interaction, the patterns described above move slowly and retain their own structure. We can easily obtain the equations for their coordinates and phases. However, prior to derivation of these equations we will modify the formulation of the problem. We will consider the dynamics of structures in a region $\Omega_1 = \{0 \le x \le L_x,\ 0 \le y \le L_y\}$ with periodic boundary conditions along both coordinates instead of an infinitely long band of width L_y. Then the energy of interaction of the strip and the ith spiral will depend not only on the distance $|x_1 - x_{0i}|$ but also on $L_x - |x_1 - x_{0i}|$ (the points $(0, y_0)$ and (L_x, y_0) are "glued together" for periodic boundary conditions) and may be written as

$$\varepsilon_{10i} = D_1\, e^{-B|x_1 - x_{0i}|} + D_2\, e^{-B[L_x - |x_1 - x_{0i}|]}, \quad i = 1,2. \tag{24}$$

The expression for the energy of spiral interaction with one another should be modified analogously. We, however, will assume that the distance between the spirals, r_{12}, is much smaller than the characteristic size of the box. Then the additional terms in the expression for ε_{012} may be neglected. The expression (24) is also valid for the box unbounded along x (i.e., a band of width L_y) if the spirals interact not with one but with two strips that bound the region of spiral localization and are at a distance L_x from one another.

We will use the variational form of Eq. (12) for the derivation of the equations of motion for spirals and strips. We will have

$$\sum_{ij} \int_{\Omega_1} (\partial_{s_i} w)\dot{s}_i (\partial_{s_j} w)\delta s_j \,\mathrm{d}^2\boldsymbol{r} = -\sum_j \frac{\partial V}{\partial s_j}\delta s_j, \tag{25}$$

where $(s_1, \ldots, s_8) = (x_{01}, y_{01}, \psi_{01}, x_{02}, y_{02}, \psi_{02}, x_1, \psi_1)$. From (25) we immediately find

$$M_{ij}\dot{s}_i = -\frac{\partial V}{\partial s_j}, \quad M_{ij} = \int_{\Omega_1} (\partial_{s_i} w)(\partial_{s_j} w)\,\mathrm{d}^2\boldsymbol{r}. \tag{26}$$

We assume, again, that the spirals and the strips are rather far apart. Then the matrix M disintegrates into three matrices: two 3×3 matrices

$$M^{(i)} = \begin{pmatrix} A_1 & m_i\gamma & 0 \\ m_i\gamma & A_2 & 0 \\ 0 & 0 & A_3 \end{pmatrix} e^{2\psi_{0i}}, \quad i = 1,2, \tag{27}$$

which describes the dynamics of spirals, and a 2×2 matrix

$$M^{(3)} = \begin{pmatrix} B_1 & 0 \\ 0 & B_2 \end{pmatrix} e^{2\psi_1}, \tag{28}$$

that describes the dynamics of the strips. Here we have

$$A_1 = \int_{\Omega_1} \left[\partial_x \left(e^{-cm_i\varphi}\, \overline{w}_0(r)\right)\right]^2 d^2\boldsymbol{r},$$

$$A_2 = \int_{\Omega_1} \left[\partial_y \left(e^{-cm_i\varphi}\, \overline{w}_0(r)\right)\right]^2 d^2\boldsymbol{r},$$

$$A_3 = \int_{\Omega_1} \left[e^{-cm_i\varphi}\, \overline{w}_0(r)\right]^2 d^2\boldsymbol{r},$$

$$\gamma = \frac{1}{m_i}\int_{\Omega_1} \left[\partial_x \left(e^{-cm_i\varphi}\, \overline{w}_0(r)\right)\right]\left[\partial_y \left(e^{-cm_i\varphi}\, \overline{w}_0(r)\right)\right] d^2\boldsymbol{r} \tag{29}$$

and

$$B_1 = \int_{\Omega_1} [\partial_x \overline{w}_1(x)]^2\, d^2\boldsymbol{r},$$

$$B_2 = \int_{\Omega_1} [\overline{w}_1(x)]^2\, d^2\boldsymbol{r}. \tag{30}$$

Note that (29) coincide with the expressions derived in [13] in the analysis of the interaction of two isolated spirals. Below we will use the result obtained in [13] according to which A_i and γ do not depend on the topological charge of the spiral and A_i are positive.

Consider the equations of motion for the strip

$$\begin{aligned} e^{2\psi_1} B_1 \dot{x}_1 &= -\partial_{x_1} V = -e^{\psi_1+\psi_{01}}\, \partial_{x_1}\varepsilon_{101} - e^{\psi_1+\psi_{02}}\, \partial_{x_1}\varepsilon_{102}, \\ e^{2\psi_1} B_2 \dot{\psi}_1 &= -\partial_{\psi_1} V = -2\, e^{2\psi_1}\, \varepsilon_1 - e^{\psi_1+\psi_{01}}\, \varepsilon_{101} - e^{\psi_1+\psi_{02}}\, \varepsilon_{102}. \end{aligned} \tag{31}$$

From (30) follows that the "masses" of the strip are $B_i \sim L_y$. Since there is exponentially weak dependence of the strip–spiral interaction energy ε_{10i} on L_y, for $L_y \gg 1$, we have $\dot{x}_1 = 0$. The latter means that the strip whose "mass" is much larger than the 'masses" of the spirals remains motionless in the interaction. On the other hand, the self-energy ε_1 of the strip, as well as its "mass", are proportional to L_y. Therefore from the second equation in (31) we find

$$\psi_1 = -(2\varepsilon_1/B_2)t + \psi_1^{(0)}. \tag{32}$$

By employing (22), (26), and (31) we can easily derive equations for the phase differences of the strip and spirals:

$$\partial_t(\psi_{02} - \psi_{01}) = 2\omega_{012} sh(\psi_{02} - \psi_{01}) + [\omega_{101} \exp(\psi_1 - \psi_{01}) - \omega_{102} \exp(\psi_1 - \psi_{02})]$$
$$\partial_t(\psi_1 - \psi_{0i}) = 2(\omega_0 - \omega_1) + \omega_{10i} \exp(\psi_1 - \psi_{0i}) + \omega_{012} \exp(\psi_{0j} - \psi_{0i}), \quad i \neq j, \tag{33}$$

where $\omega_0 = \varepsilon_0/A_3$, $\omega_1 = \varepsilon_1/B_2$, $\omega_{10i} = \varepsilon_{10i}/A_3$, and $\omega_{012} = \varepsilon_{012}/A_3$. The system (33) has a stationary solution

$$\delta = \psi_{02} - \psi_{01} = \ln \frac{2(\omega_1 - \omega_0) + \omega_{012}\omega_{101}/\omega_{102}}{2(\omega_1 - \omega_0)\omega_{101}/\omega_{102} + \omega_{012}},$$
$$\Delta_i = \psi_1 - \psi_{0i} = \ln \left[\left(2\omega_1 - 2\omega_0 - \omega_{012} e^{\pm\delta}\right)/\omega_{10i}\right], \tag{34}$$

where $+\delta$ corresponds to $i = 1$ and $-\delta$ to $i = 2$. The negative interaction energies $\varepsilon_{012} < 0$, $\varepsilon_{10i} < 0$ $(i = 1,2)$, and $\omega_{012} > 2(\omega_1 - \omega_0)$ are the sufficient conditions of stability of the solution (34). Under these conditions, the interacting structures are fully synchronized: the phase differences of the spirals and strips cease to depend on time. If $\varepsilon_{101} = \varepsilon_{102}$, then from (33) follows $\delta = 0$ and $\Delta_1 = \Delta_2$. In other words, both frequency and phase locking occur.

Thus, a stable regime of complete synchronization of structures sets in under certain conditions in the system that consists of a strip and two spirals interacting with one another.

We will investigate the relative position of spiral pairs and strips supposing the structures to be synchronized. To this end, we will consider the equation of motion for the coordinates of spiral cores:

$$(A_1A_2 - \gamma^2)\dot{x}_{0i} = [m_i\gamma\partial_{y_{0i}}\varepsilon_{012} - A_2\partial_{x_{0i}}\varepsilon_{012}]\, e^{\pm\delta} - A_2\partial_{x_{0i}}\varepsilon_{10i}\, e^{\Delta_i},$$
$$(A_1A_2 - \gamma^2)\dot{y}_{0i} = [m_i\gamma\partial_{x_{0i}}\varepsilon_{012} - A_1\partial_{y_{0i}}\varepsilon_{012}]\, e^{\pm\delta} + m_i\gamma\partial_{x_{0i}}\varepsilon_{10i}\, e^{\Delta_i}, \tag{35}$$

where $A_1A_2 - \gamma^2 > 0$ in accord with the Cauchy–Schwartz inequality. We will assume that the energy of interaction of the strip with the ith spiral, $\varepsilon_{10i}(|x_1 - x_{0i}|)$, is the function that reaches its minimum at $|x_1 - x_{0i}| = L_x/2$ (see (24)) that is symmetric relative to this point and has no other extremums in the domain $x \in [0, x_1) \cup (x_1, L_x]$. We will specify the problem and consider the interaction of two spirals having opposite charges: $m_1 = -m_2$. Such a pair is called a dipole. We choose the dipole–strip interaction for analysis because the summary topological charge of defects in a system with periodic boundary conditions must be equal to zero. Because in the interaction with the spirals the strip remains motionless, we can assume, without loss of generality, $x_1 = 0$ and consider, for simplicity, that the spirals which are equidistant from the strip $x_{01} = L_x - x_{02}$ assuming $x_{01} \neq x_{02}$ and $y_{01} \neq y_{02}$. Then $\varepsilon_{101} = \varepsilon_{102}$, $\partial_{x_{01}}\varepsilon_{101} = -\partial_{x_{02}}\varepsilon_{102}$, $\delta = 0$, $\Delta_1 = \Delta_2 = \Delta$, and for the difference of the coordinates of the spirals we have

$$(A_1A_2 - \gamma^2)\partial_t(x_{02} - x_{01}) = -2A_2(\partial_{x_{02}}\varepsilon_{012} + \partial_{x_{02}}\varepsilon_{102} e^{\Delta}),$$
$$(A_1A_2 - \gamma^2)\partial_t(y_{02} - y_{01}) = -2A_1\partial_{y_{02}}\varepsilon_{012}, \tag{36}$$

In the reference system moving with the dipole's "center of mass", the spiral motion consists of the turn relative to the "center of mass" and displacement along the dipole axis. It follows from (36) that such a motion transforms the system to the stable state $x_{01} = x_{02} = L_x/2$, $|y_{01} - y_{02}| = R_0$ where R_0 is the distance between the spirals that corresponds to the minimal interaction energy ε_{012} (see Section 2). The spiral motion in the "center of mass" reference system is accompanied by the displacement of the "center of mass" itself along the y-axis, with the direction of the displacement being determined by the sign of γ (see (35)). In a general case, when the "center of mass" does not originally belong to the straight line $x = L_x/2$, the spiral motion is qualitatively different but it is accompanied by the displacement of the "center of mass" of the spiral pair both along the y- and the x-axes and also results in the equilibrium state.

There is an important circumstance which we would like to emphasize. Consider a pair of spirals located at different distances from the strips assuming $\omega_{10i} > \omega_{10j}$. Suppose that the sufficient stability conditions $\omega_{012} < 0$, $\omega_{10i} < 0$, $\omega_{012} > 2\ (\omega_1 - \omega_0)$ are fulfilled for the synchronization regime. Then we can readily verify that $\Delta_i > \Delta_j$ and $\psi_{0j} > \psi_{0i}$. Consequently, the ith spiral possessing the highest energy (i.e., the spiral that is the closest to the strip) moves with a velocity greater than the velocity of the jth spiral. The difference is the greater, the larger the coefficients $e^{\psi_{0j}-\psi_{0i}}$ and e^{Δ_i} compared to the corresponding coefficients $e^{\psi_{0i}-\psi_{0j}}$ and e^{Δ_j} in the right-hand side of (35). Thus the dipole, that was originally turned relative to the strip axis, tends to be arranged in parallel to this axis. This allows us to suppose that, in spite of exponentially weak interaction, the dipole is quite rapidly arranged regularly with respect to the strip even when the dipole and the strip are spaced rather far apart.

Thus, we have shown that the interaction of a pair of the spirals having opposite topological charges ($m_1 = -m_2$) with one another and with a strip may give rise to their frequency and phase locking and in the formation of the equilibrium state in which the spirals are located along a straight line parallel to the axis of the strip.

In the system consisting of a great number of spirals interacting with one another and with strips, the synchronization regime means the transition from defect mediated turbulence to a one-dimensional (along y) spatial disorder of spiral dipoles periodically oscillating in time. Finally, in the system containing a great number of spirals and strips located at arbitrary distances from one another, the synchronization means the onset of a two-dimensional spatial disorder also periodically varying in time. In this case, the distribution of the field amplitude is time invariant and contains a set of randomly spaced spiral pairs parallel to the strip axes. Note that in the system containing many strips located at random distances from one another, the minimal energy of the interaction of the spirals with two neighboring strips is not necessarily located exactly in the middle between them. This is explained by the fact that the location of the minima depends not only on the nearest but also on other strips in the system.

4. Numerical experiment

The interaction of the structures was investigated in the frames of Eq. (1) integrated following the scheme described above in the domain with periodic boundary conditions. The field distribution in the 150×150 square at $\alpha = 0.2$ and $\beta = 2$ is shown in Fig. 2. The distribution containing a strip and chaotically spaced spirals was taken as the initial condition. It is worth noting that the spirals are rather rapidly arranged along a straight line (in several hundred time units), in spite of exponentially weak interaction. On completion of this process, the spiral chain, actually, does not change its position relative to the strip. A similar picture is observed in the 600×80 band. A typical field distribution at $\alpha = 0.2$ and $\beta = 2$ is depicted in Fig. 3. It is clearly seen that the spiral dipoles are always arranged parallel to the stip axis. The snapshot of the field at other values of the parameters $\alpha = 0.1$ and $\beta = 2$ is given in Fig. 4. In this case, the spirals are not synchronized in space, instead, each of them retains its own dynamics. It is to be noted, however, that the spirals are localized in the region the boundaries of which are spaced from the strips at a distance that is

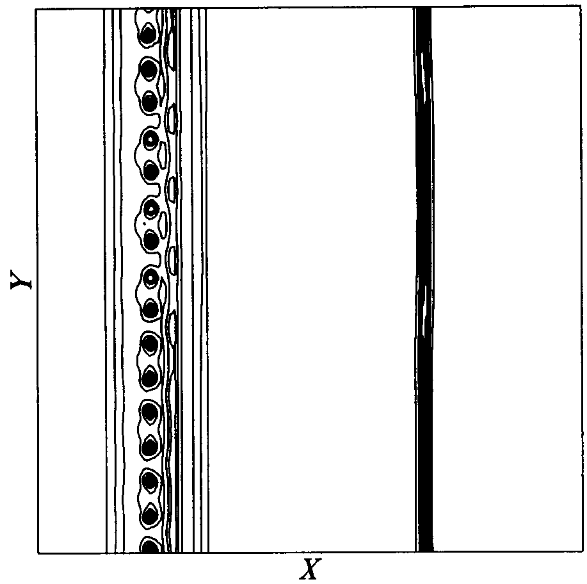

Fig. 2. Level lines of the amplitude of established field distribution for $\beta = 2$ and $\alpha = 0.2$ in the 150×150 square. A regular distribution of the spirals demonstrates the effect of spatio-temporal organization under random initial conditions.

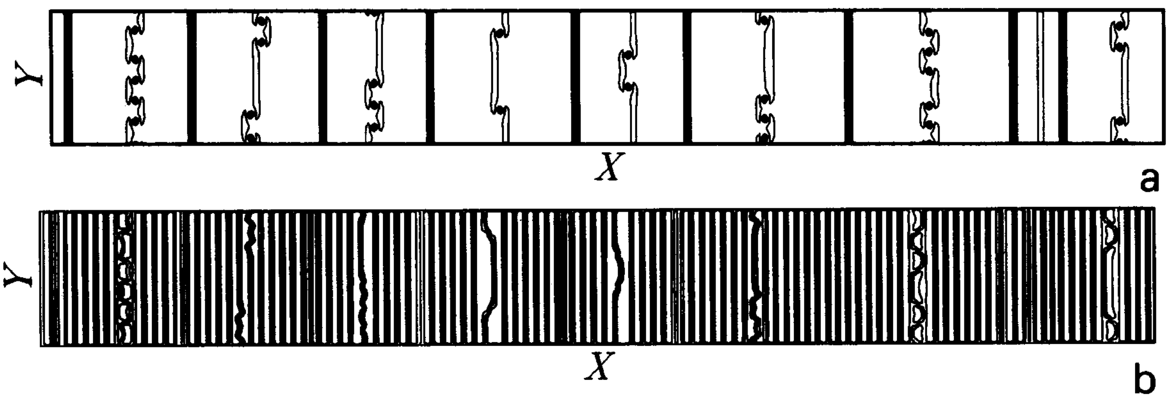

Fig. 3. Level lines of the amplitude (a) and real part (b) of established field distribution for $\beta = 2$ and $\alpha = 0.2$ in the 600×80 band. A regime of spatial disorder periodically oscillating in time is established when the spiral dipoles are arranged parallel to the strip axes and have random (time invariable) coordinates along the y-axis.

several times greater than the size of the strip cores. When the neighboring spirals are rather close to one another, the spirals located between them have an almost regular distribution in the form of a chain parallel to the strip axes. Note that the initial distribution depicted in Fig. 4 for $\alpha = 0.2$ and $\beta = 2$ evolves to a regular distribution like the one shown in Fig. 3.

The collective behavior of the spirals localized in the region bounded by two parallel strips can be easily understood by drawing an analogy with particles in a potential well. As long as the self-energy (kinetic energy) of the spirals is small compared to the "depth" of the well, the spirals are located at its bottom, i.e., at the potential energy minimum (see Figs. 2, 3). When the self-energy of the spirals is comparable with the depth of the well, the spirals have chaotic dynamics throughout the well except the narrow regions near the strips where the interaction energy increases sharply

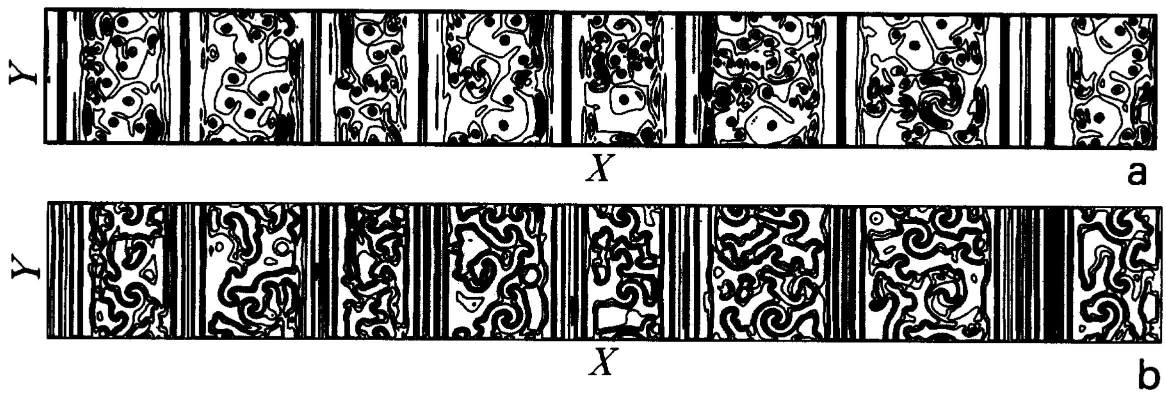

Fig. 4. Snapshots of the amplitude (a) and real part (b) of the field for $\beta = 2$ and $\alpha = 0.1$ in the 600×80 band. Several space-localized turbulent spots bounded by parallel strips are clearly seen.

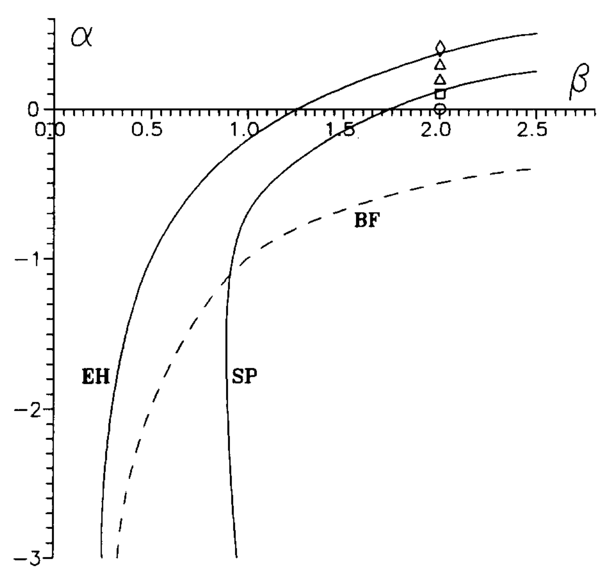

Fig. 5. The plane of the parameters α and β. Presented are the Benjamin–Fair limit (dotted line, BF); the long wavelength Eckhaus limit with $Q(\alpha, \beta)$ corresponding to 2D spirals (solid line, EH); and the absolute stability limit for 2D spirals (solid line, SP) [5,18]. Marked are the values of the parameters corresponding to the regimes observed: (○) developed defect mediated turbulence, the strips are destroyed; (□) defect mediated turbulence in the region between stable strips (see Fig. 4); (△) spatio-temporal organization of spirals in the region between stable strips (Figs. 2,3); (◇) quasistationary spatial disorder of spirals, the strips are destroyed.

(Fig. 4). With a still further increase of the self-energy (due to the variation of α and β), the spirals tend to escape from the potential well. As a result, the strips break and the region of spiral localization extends to the entire space. Typical values of the parameters α and β to which different regimes of co-existence of spirals and strips correspond are presented in Fig. 5.

5. Dynamics of circular strips

Let us come back again to the Ginzburg–Landau equation (1) and write it down in a polar coordinate system:

$$\partial_t a = a - (1 + i\beta)|a|^2 a + (1 + i\alpha)\left(\partial_{rr}^2 a + \frac{1}{r}\partial_r a + \frac{1}{r^2}\partial_{\varphi\varphi}^2 a\right) \tag{37}$$

One can readily see that, for $r \gg 1$, the contribution of two last terms in the expression for the Laplacian is small and tends to zero as $r \to \infty$. The latter allows us to suppose that Eq. (37) will have a solution in the form

$$a = A(r - r_0)\exp[-i\omega t + i\theta(r - r_0)] + \mathcal{O}(1/r_0), \quad r_0 \gg 1, \tag{38}$$

where the amplitude A and phase θ satisfy (6) and (7) in which $r - r_0$ must be substituted for x. For $|r - r_0| \gg 1$, the solution (38) tends asymptotically to the solution in the form of a cylindrical wave with the wavenumber Q. Thus, for $r \gg r_0 \gg 1$, (38) behaves as a spiral with a topological charge $m = 0$. On the other hand, it can be expected that the cylindrical waves radiated inwards the circular strip (38) will be absorbed by a shock structure. This supposition is confirmed by results of numerical experiment (see the text below).

We will investigate the effect of small perturbations introduced by the components $(1/r)\partial_r$ and $(1/r^2)\partial_{\varphi\varphi}^2$ of the Laplacian on the dynamics of the solution (38). Let us again employ Eq. (11). In the new variables the solution (38) takes on the form

$$w^{(0)}(r - r_0) = [ch[k(r - r_0)]]^{-B/k}\,e^{\psi_0} \tag{39}$$

(where ψ_0 is an arbitrary constant). It is an exact solution to the unperturbed (in the sense $\nabla^2 = \partial_{rr}^2$) equation (11).

We will seek a solution to the perturbed (complete) equation (11) in the form

$$w(r,t) = \{ch[k(r - r_0(\varepsilon t))]\}^{-B/k}\,e^{\psi_0(\varepsilon t)} + \sum \varepsilon^n w^{(n)}, \tag{40}$$

where the small parameter is $\varepsilon \sim 1/r$, and $r_0(\varepsilon t)$ and $\psi_0(\varepsilon t)$ are the slow functions of time. By substituting (40) into (11) and equating the terms for different power exponents of ε we obtain a system of linear differential equations

$$\varepsilon^n[\partial_t w^{(n)} - (1 + \alpha\beta)(\partial_{rr}^2 w^{(n)} - B^2 w^{(n)})] = H^{(n)}, \tag{41}$$

where $H^{(n)}$ is the expression that contains corrections from the previous orders of approximation and does not include $w^{(n)}$. It is known that the nonuniform system (41) has bounded solutions if its right-hand side is orthogonal to the eigenfunctions of the system conjugate to the homogeneous system. The linear operator $\hat{L}$ in the left-hand side of (41) with the domain $D(\hat{L}) = \{w : w \in \mathbb{C}^2;\ w(r) \to 0,\ r \to \infty;\ \partial_r w(r_c) = 0\}$ is self-conjugate in the space of the functions that are continuous on the interval $r \in [r_c, \infty)$ where $0 < r_c \ll r_0$. Because $w^{(0)}$ and $\partial_r w^{(0)}$ are the solutions of a uniform equation and

$$H^{(1)} = \partial_r w^{(0)}\dot{r}_0 + w^{(0)}\dot{\psi}_0 + (1 + \alpha\beta)\frac{1}{r}\partial_r w^{(0)}, \tag{42}$$

from the orthogonality condition to the first approximation we have

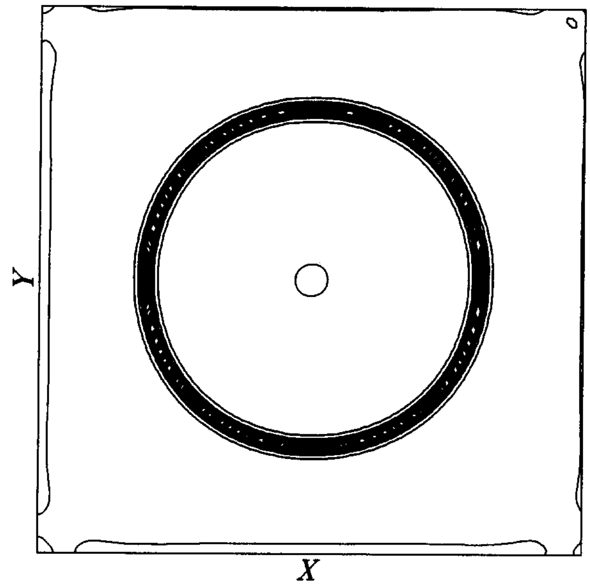

Fig. 6.

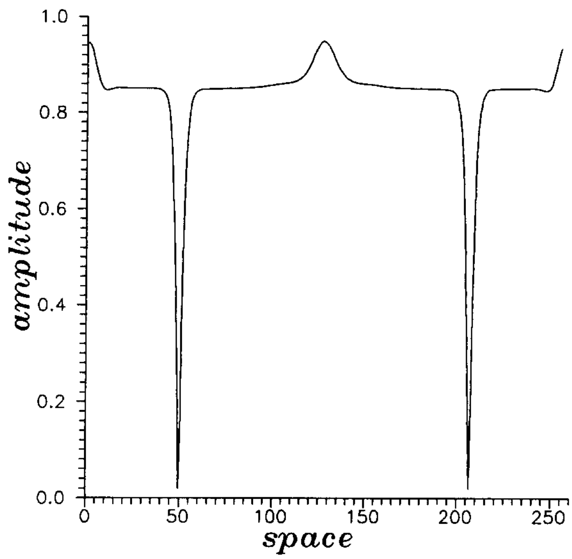

Fig. 7.

Fig. 6. A snapshot of the field amplitude for $\beta = 2$ and $\alpha = 0.2$ in the 75×75 square. The radius of the circular strip is slowly decreasing in time, with the rate of this process being the faster the smaller the radius.

Fig. 7. The longitudinal structure of the field for $y = L_y/2$ corresponding to the snapshot presented in Fig. 6. Well seen are the shocks, one of which is located at the center of the circular strip ($x = y = L_x/2$).

$$\dot{r}_0 \int_{r_c}^{\infty} (\partial_r w^{(0)})^2 \, \mathrm{d}r = -(1 + \alpha\beta) \int_{r_c}^{\infty} \frac{1}{r} (\partial_r w^{(0)})^2 \, \mathrm{d}r, \quad \dot{\psi}_0 = 0. \tag{43}$$

From the first equation of the system (43) follows $\dot{r}_0 < 0$, i.e., the radius r_0 of the solution (38) decreases. Besides, one can readily verify that at $r_0 \to \infty$ we have

$$\int_{r_c}^{\infty} \frac{1}{r} (\partial_r w^{(0)})^2 \, \mathrm{d}r \to 0$$

and, consequently, $\dot{r}_0 \to 0$. Thus, as $r_0 \to \infty$, the lifetime of the solution (38) increases without restriction [1].

Numerical investigations confirm the result obtained. Eq. (1) was integrated in the 300×300 and 150×150 domains with periodic boundary conditions for 512×512 and 256×256 FFT harmonics. A snapshot of the field is shown in Fig. 6 for $\alpha = 0.2$ and $\beta = 2$. The corresponding longitudinal structure of the field ($y = L_y/2$) is presented in Fig. 7. It is clearly seen that a shock structure absorbing the waves radiated inwards the strip is formed at the center ($x = y = L/2$) even in the absence of spirals. The distribution containing several strips enclosed into one another (Fig. 8) is also possible but at other initial conditions. The radius of the circular structures depicted in Fig. 8 decreases with time and they vanish one after another. Fig. 9 presents the snapshot of

[1] It should be emphasized that we do not investigate stability of the solution (38) with respect to the perturbations of the solution per se.

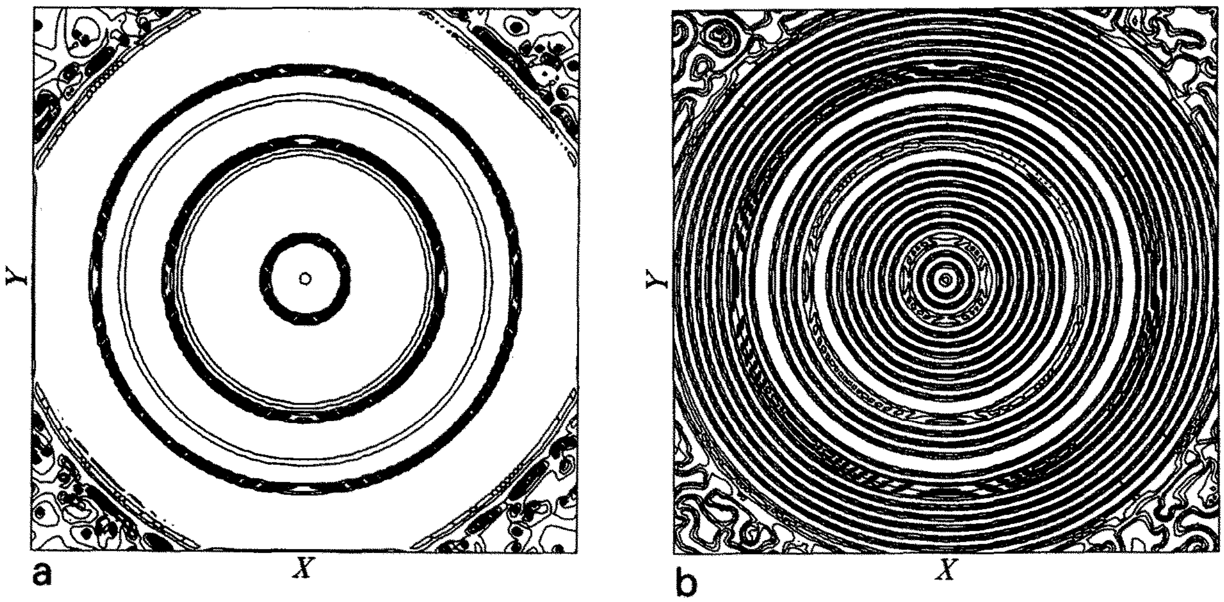

Fig. 8. Snapshots of the amplitude (a) and real part (b) of the field for $\beta = 2$, $\alpha = 0.2$ and $T = 700$. A few circular strips enclosed one into another, with the radii slowly decreasing in time, stably co-exist in the 300×300 square.

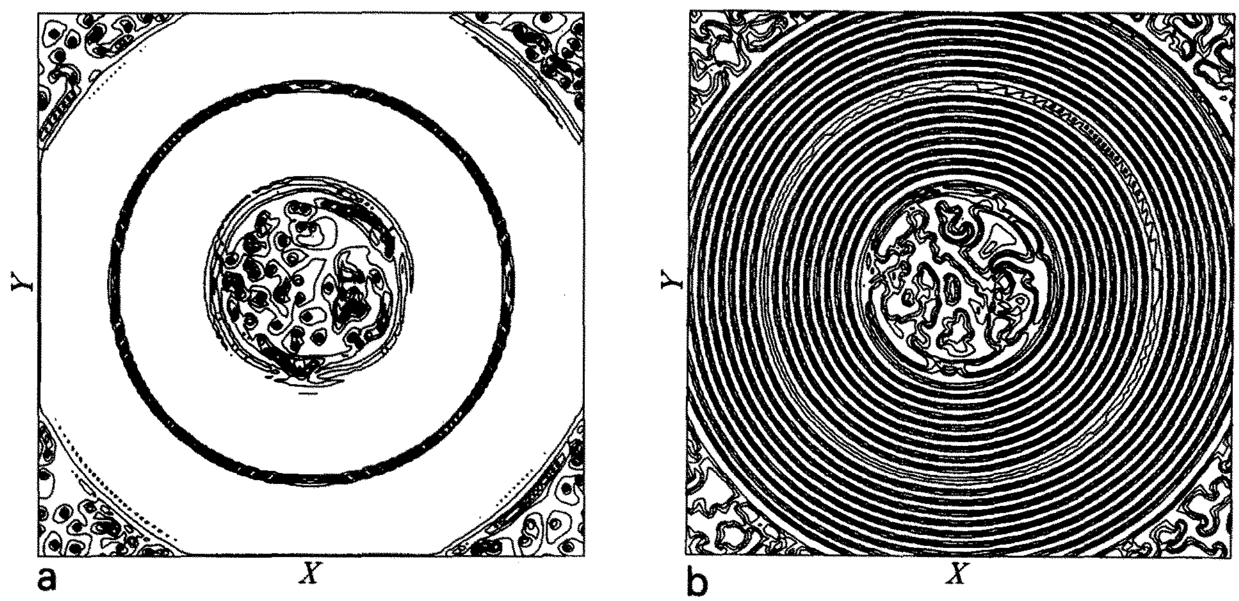

Fig. 9. Time evolution of the spatial distribution presented in Fig. 8 ($T = 1600$). Depicted are the amplitude (a) and real part (b) of the field. As the circular strips of small radii are disappearing, a turbulent spot containing the spirals chaotically arranged in space are formed in the region bounded by an external strip.

the field corresponding to the further evolution of the spatial distribution shown in Fig. 8. It is interesting that a great number of spiral pairs are born as the inner strips "are collapsing" in the region bounded by a circular strip of maximal radius (see Fig. 9). As the outer strip is constricted, the localization region of the spirals decreases, they are partially ordered in space (Fig. 10) and,

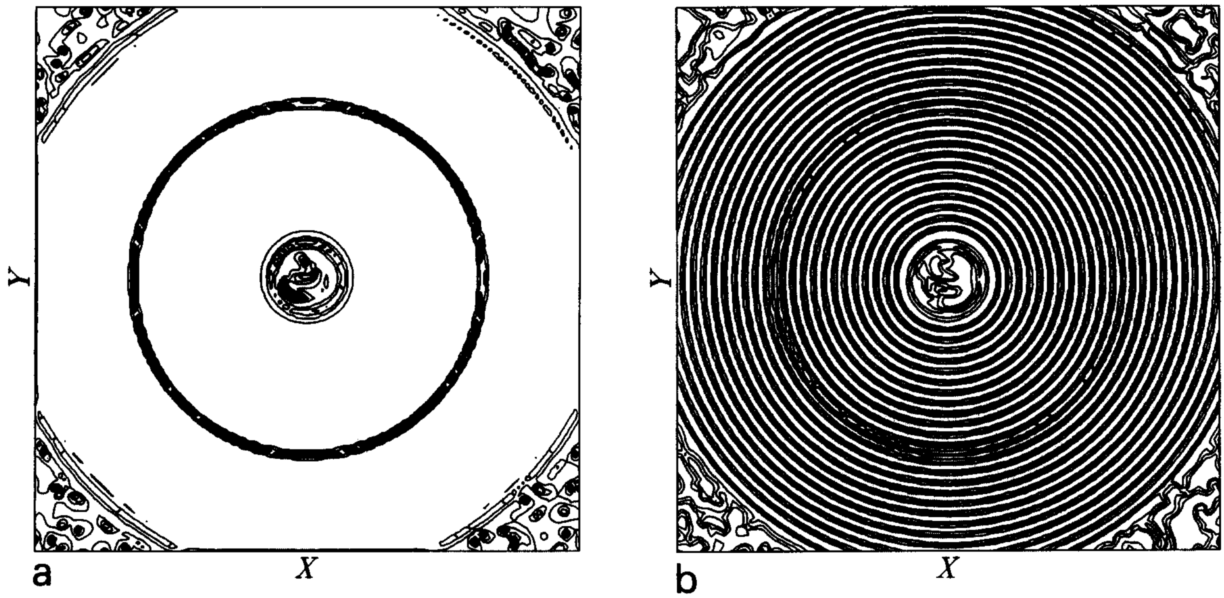

Fig. 10. Snapshots of the amplitude (a) and real part (b) of the field corresponding to further evolution of the spatial distribution depicted in Fig. 9 ($T = 2800$). As the region of spiral localization is decreased due to the contraction of the strips, the spirals are partially ordered in space (arranged around a circumference) and then disappear as a result of pair annihilation.

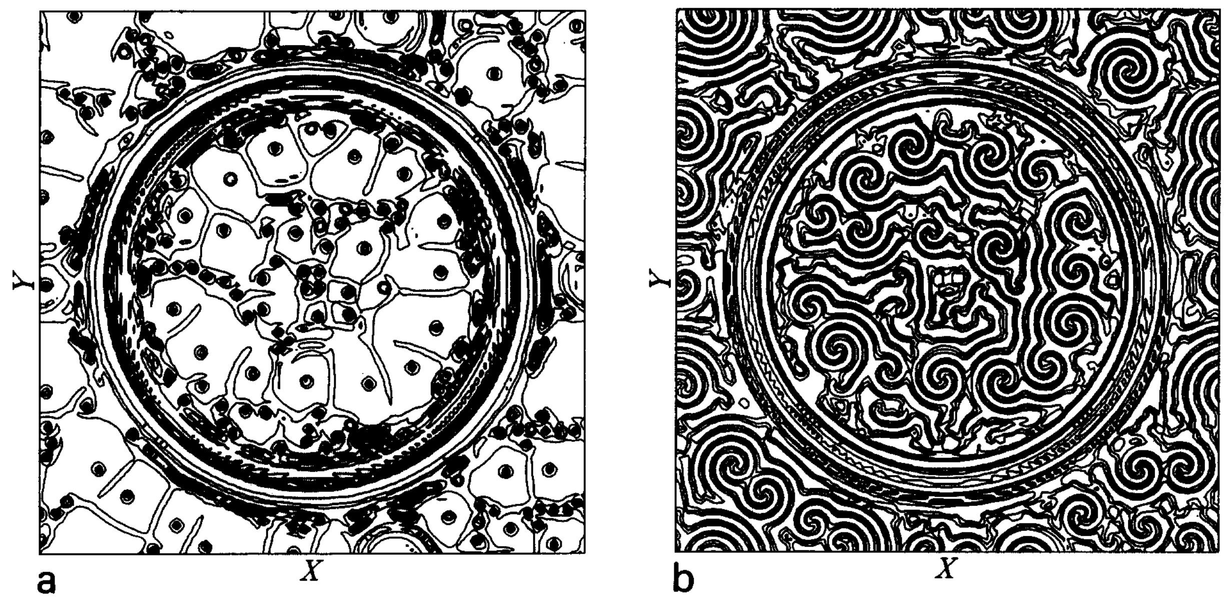

Fig. 11. Snapshots of the amplitude (a) and real part (b) of the field for $\beta = 1.7$ and $\alpha = 0$. The spirals fill the entire region (300×300 square) including the neighborhood of the core of the strip (cf. Fig. 9).

finally, they all annihilate in pairs. The shapshot of the field for other values of the parameters ($\alpha = 0$ and $\beta = 1.7$) is shown in Fig. 11. The radius of the circular strip in this case is slowly decreasing with time but the region of spiral localization inside the strip is much larger than in the analogous situation depicted in Fig. 9. It should be noted that, as was verified in numerical experiment, the solutions (38) retain their circular structure throughout their lifetime down to the strip width $r_0 \sim d$.

6. Conclusion

When speaking about spatio-temporal patterns in extended systems researchers usually analyse three groups of problems (see, for example, [49–51]): (1) the patterns ordered in space and time (e.g., living or frozen crystals or quasicrystals, travelling or standing waves); (2) irregular in space but time-independent patterns (frozen disorder); and (3) the patterns irregular both in space and time (spatio-temporal chaos). The results presented in this paper show that extended systems may also demonstrate a different and slightly unexpected behavior that is chaotic in space and periodically varying in time. Stable existence of such a disorder is a result of the synchronization phenomenon. The characteristics of the "periodically oscillating disorder" (generalized dimensions or densities of dimensions, the Kolmogorov entropy, etc.) are still to be investigated. We believe that one of the most important problems to be studied is the transition from the time-periodic disorder to spatio-temporal chaos. Preliminary computer experiments indicate that this transition occurs inhomogeneously in space demonstrating a specific form of intermittency.

In conclusion we would like to emphasize that the results presented above were obtained under the supposition that the strip solutions do not decay in the course of development of instabilities. The hole solutions are known [10] to be neutrally stable in a one-dimensional CGLE. Moreover, they may become stable if an additional nonlinearity, for example, $\sim|a|^4 a$ is taken into account in the CGLE. Such nonlinearity may be induced, in particular, by the numerical scheme used in computer experiment. In the formulation of the problem considered here, the situation may be even more favourable for strip stability. It is highly probable that the strips will additionally stabilize one another due to periodic boundary conditions.

We would like to add that the problem of strip stability is essential for understanding the mechanisms responsible for the existence of different types of defect mediated turbulence and needs further investigation.

7. Acknowledgements

We highly appreciate fruitful discussions with K.A.Gorshkov. This research was supported by the Russian Foundation of Fundamental Research (grant N 93–02–15424, grant N 94-02-03263-a).

References

[1] M. Bazhenov and M. Rabinovich, Phys. Lett. A 179 (1973) 191.
[2] K. Nozaki and N. Bekki, J. Phys. Soc. Jpn. 53 (1984) 1581.
[3] K. Nozaki and N. Bekki, Phys. Lett. A 110 (1985) 133.
[4] H. Sakaguchi, Prog. Theor. Phys. 83 (1990) 169.
[5] A. Weber, L. Kramer, I.S. Aranson and L. Aranson, Physica D 61 (1992) 279.
[6] H. Sakaguchi, Prog. Theor. Phys. 85 (1991) 417.
[7] W. Saarloos and P.C. Hohenberg, Physica D 56 (1992) 303.
[8] H. Chate and P. Manneville, Phys. Lett. A 171 (1992) 183.

[9] S. Sasa and T. Iwamoto, Stability of Phase-Singular Solutions to the One-Dimensional Complex Ginzburg–Landau Equation, unpublished.
[10] I. Aranson, L. Kramer, S. Popp, O. Stiller and A. Weber, Phys. Rev. Lett. 70 (1993) 3880.
[11] Y. Kuramoto and S. Koga, Prog. Theor. Phys. 66 (1981) 1081;
Y. Kuramoto, Chemical Oscillations, Waves and Turbulence (Springer, Berlin, 1984).
[12] E. Bodenschatz, M. Kaizer, L. Kramer, W. Pesch, A. Weber, and W. Zimmermann, in: New Trends in Nonlinear Dynamics and Pattern Forming Phenomena, P. Coullet and P. Huerre, eds. (Plenum, New York, 1990) p. 111.
[13] I.S. Aranson, L. Kramer and A. Weber, Physica D 53 (1991) 376.
[14] S. Rica and E. Tirapegui, Physica D 48 (1991) 396.
[15] A.A. Nepomnyashchy and L.M. Pismen, Phys. Lett A 153 (1991) 427.
[16] J.D. Rodriguez, L.M. Pismen and L. Sirovich, Phys. Rev. A 44 (1991) 7980.
[17] L.M. Pismen and A.A. Nepomnyashchy, Physica D 54 (1992) 183.
[18] I.S. Aranson, L. Aranson, L. Kramer and A. Weber, Phys. Rev. A 46 (1992) R 2992.
[19] G. Huber, P. Alstrøm and T. Bohr, Phys. Rev. Lett. 69 (1992) 2380.
[20] C. Matsuoka and K. Nozaki, J. Phys. Soc. Jpn. 61 (1992) 1429.
[21] I.S. Aranson, L. Kramer and A. Weber, Phys. Rev. E 47 (1993) 3231.
[22] I.S. Aranson, L. Kramer and A. Weber, Phys. Rev. E 48 (1993) R 9.
[23] I. Aranson, L. Kramer and A. Weber, submitted to Phys. Rev. Lett.
[24] L.M. Pismen and J. Rubinstein, Physica D 47 (1991) 353.
[25] H. Sakaguchi, Prog. Theor. Phys. 84 (1990) 792.
[26] M. Bartuccelli, P. Constantin, C.R. Doering, J.D. Gibbon and M. Gisselfalt, Physica D 44 (1990) 421.
[27] L. Gil, Nonlinearity 4 (1991) 1213.
[28] B.I. Shraiman, A. Pumir, W. Saarloos, P.C. Hohenberg, H. Chate and M. Holen, Physica D 57 (1992) 241.
[29] M.V. Bazhenov, A.L. Fabrikant and M.I. Rabinovich, Phys. Lett. A 163 (1992) 87.
[30] H. Chaté, in: Proc. of the KIT Int. Workshop on the Physics of Pattern Formation in Complex Dissipative Systems, S. Kai, ed. (World Scientific, Singapore, 1992) p. 374.
[31] P. Coullet, L. Gil and J. Lega, Physica D 37 (1989) 91; Phys. Rev. Lett. 62 (1989) 1619.
[32] J.-L. Meunier, in: New Trends in Nonlinear Dynamics and Pattern Forming Phenomena, P. Coullet and P. Huerre, eds. (Plenum, New York, 1990) p.181.
[33] G. Huber and P. Alstrøm, Physica A 195 (1993) 448.
[34] M.V. Bazhenov, M.I. Rabinovich and A.L. Fabrikant, in: Proc. of the KIT Int. Workshop on the Physics of Pattern Formation in Complex Dissipative Systems, S. Kai, ed. (World Scientific, Singapore, 1992) p. 361.
[35] M.V. Bazhenov and M.I. Rabinovich, Time Periodic Spatial Disorder, unpublished.
[36] L. Sirovich and J.D. Rodriguez, Phys. Lett. A 120 (1987) 211.
[37] L. Sirovich, Physica D 37 (1989) 126.
[38] A. Doelman, Physica D 40 (1989) 156; Nonlinearity 4 (1991) 231.
[39] K. Promislow, Physica D 41 (1990) 232.
[40] W. Schöpf and L. Kramer, Phys. Rev. Lett. 66 (1991) 2316.
[41] M. Bestehorn, Europhysics Lett. 15 (1991) 473.
[42] S. Kishiba, S. Toh and T. Kawahara, Physica D 54 (1991) 43.
[43] M. Hirayama, H. Hirayama, M. Igai and J. Ishida, Prog. Theor. Phys. 87 (1992) 507.
[44] P. Takáč, Nonlinearity 5 (1992) 289.
[45] P.S. Hagan, SIAM J. Appl. Math. 42 (1982) 762.
[46] Y. Kuramoto and T. Tsuzuki, Prog. Theor. Phys. 55 (1976) 356.
[47] B.A. Malomed, Physica D 8 (1983) 353.
[48] S.A. Orszag, Stud. Appl. Math. 20 (1971) 293;
C. Canuto, M.Y. Hussaini, A. Quarteroni and T.A. Zand, Spectral Methods in Fluid Dynamics (Springer, Berlin, 1988).
[49] H.L. Swinney, in: Time Series, Prediction, A.S. Weigend and N.A. Gershenfeld, eds. (Addison-Wesley, New York, 1993) p. 557.
[50] V.S. Afraimovich, M.I. Rabinovich and A.L. Zheleznyak, in: Time Series, Prediction, A.S. Weigend and N.A. Gershenfeld, eds. (Addison-Wesley, New York, 1993) p. 539.
[51] M.I. Rabinovich, A.L. Fabrikant and L. Sh.Tsimring, Sov. Phys. Usp. 35 (1992) 629.